

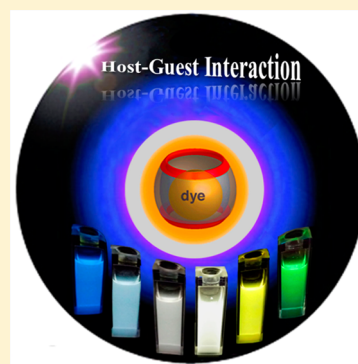
Facile Cucurbit[8]uril-Based Supramolecular Approach To Fabricate Tunable Luminescent Materials in Aqueous Solution

Xin-Long Ni,* Shiyan Chen, Yaping Yang, and Zhu Tao

Key Laboratory of Macrocyclic and Supramolecular Chemistry of Guizhou Province, Guizhou University, Guiyang, Guizhou 550025, China

S Supporting Information

ABSTRACT: Light-emitting materials with tunable properties may offer fascinating applications in optoelectronic devices, fluorescent sensors, and imaging agents. Herein, a new supramolecular approach based on host–guest interactions that greatly decreases the number of required synthetic steps and produces a system with tunable and dynamical photophysical properties was developed. Because of the novel electronic distributions of the chromophore guest within the rigid hydrophobic cavity of the cucurbit[8]uril host in this system, color tuning of emissions such as cyan, yellow, green, and white light with efficiency increased fluorescence lifetime, and quantum yield was easily achieved by simple addition of the host in aqueous solution. Stimulus-responsive tuning of color has long been an important area of research into light emissions. The current study distinguishes itself by its combination of simple steps using a single synthetic receptor and a single organic fluorophore guest in a single solution. Our results may provide a promising advancement of the fabrication of smart and tunable luminescent materials.



INTRODUCTION

Luminescent organic and organometallic molecules that can be tuned simply have attracted much attention because of their potential applications in fluorescent sensors, probes, imaging agents in biological systems,^{1–3} light-emitting diodes,⁴ and other organic electronic devices.⁵ Extending π systems^{6,7} or weakening the π – π interactions of aromatic chromophores by covalent attachment of substituents to aromatic rings⁸ has been commonly done to fabricate smart, tunable, luminescent materials. Fabrication of highly luminescent materials is efficient,^{9,10} but it often involves difficult and tedious organic synthesis with multiple steps and higher cost. In particular, fabrication of water-soluble luminescent materials is highly challenging because of the intrinsic hydrophobic effect of organic chromophores in aqueous solution. Supramolecular assembly has recently been proven to be an efficient way of fabricating smart photofunctional materials. In this method, well-ordered architectures bearing novel photophysical properties are formed spontaneously from individual chromophore components by noncovalent interaction or by self-aggregation.^{11–14} Few assemblies with optically tunable features are known.^{15–18} Nevertheless, luminescent materials based on supramolecular assemblies are attractive because of their prospects for use in advanced light-emitting materials.^{19,20}

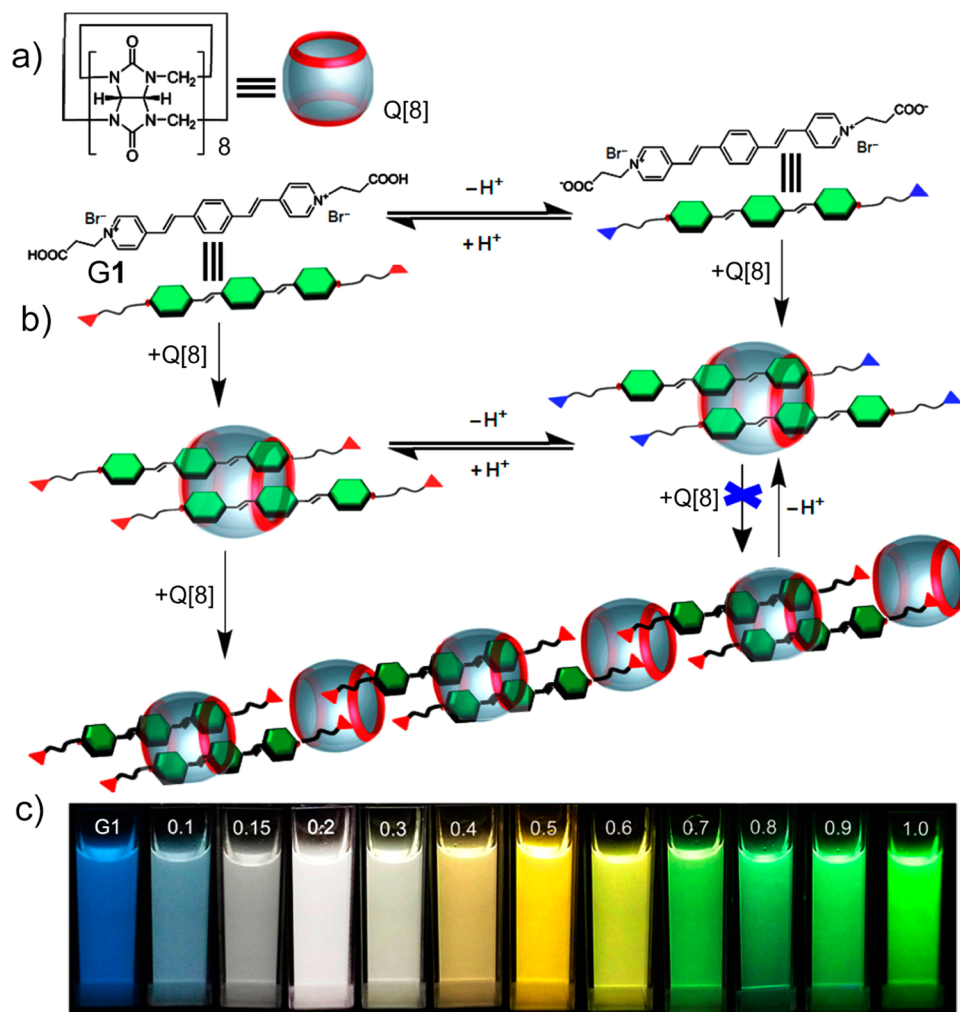
Cucurbit[n]urils (Q[n]s or CB[n]s),²¹ along with crown ethers, cryptands, cyclodextrins, and calixarenes, are macrocyclic receptors that have played a crucial role in supramolecular chemistry and materials science in recent decades.^{22,23} This popularity is due to their novel properties in the formation of inclusion complexes with various guest molecules (e.g., cationic guest) with high selectivity and a high binding

constant in aqueous solution.^{24–27} A recent study on the interactions of Q[n]s with fluorophore guest molecules was very interesting because Q[n]s can significantly modify the physicochemical properties of guest molecules upon complexation.²⁸ For example, Q[n] inclusion complexes with wholly or partially included fluorophore molecules in the hydrophobic cavities generally yield interesting luminescent properties, such as fluorescence emission with longer lifetime and higher quantum yield.^{29,30} Cucurbit[8]uril (Q[8] or CB[8]), a large homologue of the Q[n] family, is unique because of its ability to bind two hetero- and homoguests in its cavity.³¹ Through host-stabilized charge-transfer (HSCT) interactions, Q[8] can bind an electron-accepting guest and an electron-donating guest to form a Q[8]-enhanced charge-transfer complex.^{31,32} Q[8] can also accommodate two homoguests, such as naphthalene,³³ or arylpyridinium,³⁴ which can be strongly dimerized inside the cavity of Q[8] to form highly stable Q[8]-enhanced π – π complexes and, in some cases, can lead to pronounced dimer fluorescence.³⁵ Because of these features, Q[8] has been widely used in the construction of functional polymers and molecular architectures.

The linear π systems of oligo(*p*-phenylenevinylene) (OPV) dyes³⁶ make them functional chromophores that are highly useful in the design of artificial light-harvesting systems, light-emitting diodes, and supramolecular architectures.³⁷ Interestingly, the optical and electronic properties of these molecules strongly depend upon structural features. Thus, they can be modulated by variations in conjugation length and donor–

Received: February 2, 2016

Published: April 28, 2016

Scheme 1^a

^a(a) Chemical structure of Q[8] and G1. (b) Schematic representation of the Q[8]-based approach for fabricating smart luminescent materials, showing host-guest interactions of Q[8] with G1 that lead to different supramolecular assemblies in water. (c) Photographs of solution of G1 (10.0 μM) upon addition of increasing concentrations of Q[8] host (0–1.0 equiv) in aqueous media (pH 2.0) under UV light at 365 nm.

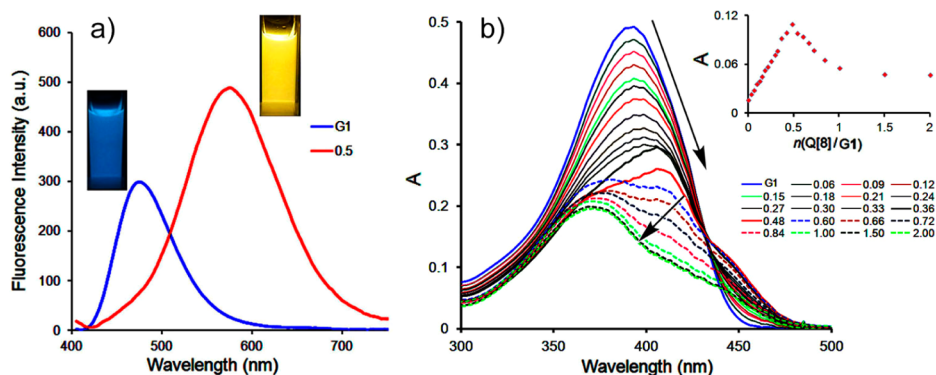


Figure 1. (a) Fluorescence emission spectrum of G1 (10.0 μM) in the absence and presence of 0.5 equiv of Q[8] host in aqueous solution (pH 2.0) ($\lambda_{\text{ex}} = 398$ nm) at 298 K. (b) UV-vis absorption spectrum of G1 (10.0 μM) at increasing concentrations of Q[8] in aqueous solution (pH 2.0) at 298 K. Inset: curve of A vs n (Q[8]/G1) for the absorption peak at 450 nm. The photophysical properties of G1 upon addition of the Q[8] container showed that the host-guest interaction strongly modified the electronic distributions of the guest within the rigid hydrophobic cavity of the Q[8] host.

acceptor strengths.^{37,38} Against this background, we anticipated that anchoring water-soluble OPV chromophores in the rigid

hydrophobic cavity of the Q[8] host would be suitable for the development of light-emitting materials.

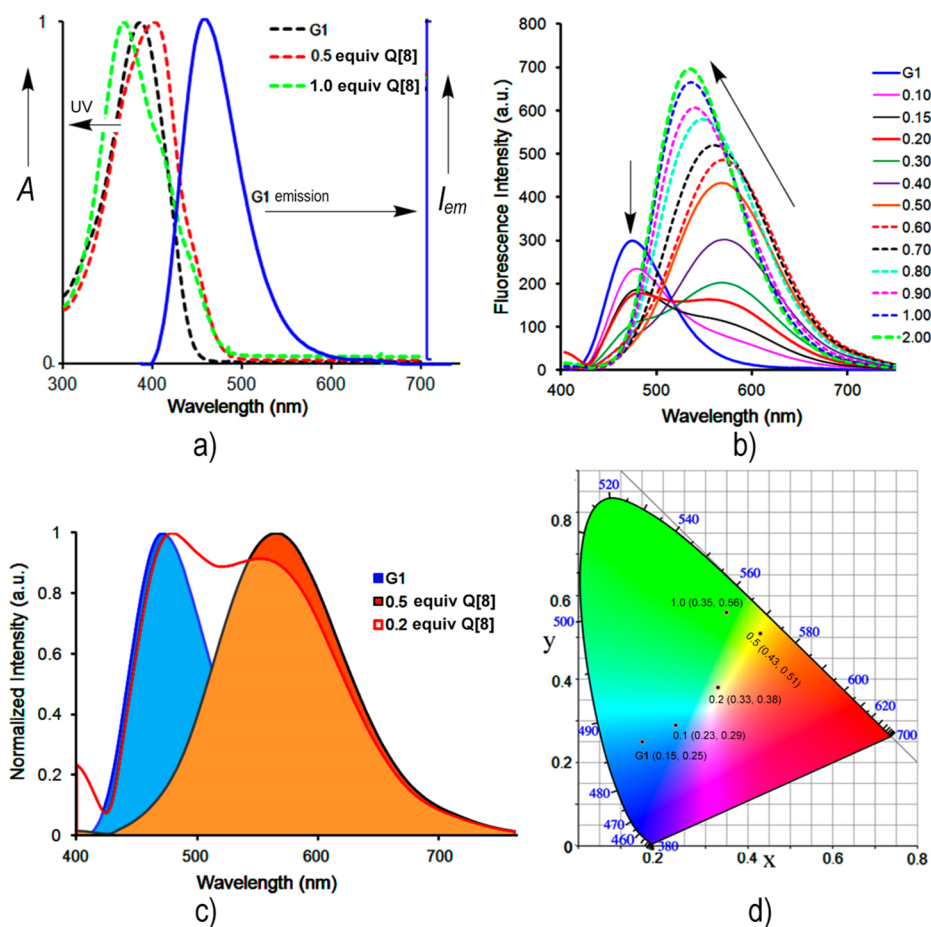


Figure 2. (a) Normalized absorption spectrum of the Q[8]-based host-guest interaction with the emission spectrum of G1 in water. (b) Changes in the fluorescence emission spectrum of G1 (10.0 μ M) upon addition of increasing concentrations of Q[8] in aqueous solution at pH 2.0 (0–2.0 equiv), $\lambda_{ex} = 398$ nm. (c) Normalized overlap fluorescence emission spectrum of G1 (10.0 μ M) with Q[8] (0.2 and 0.5 equiv) in aqueous solution (pH 2.0), $\lambda_{ex} = 398$ nm. (d) The 1931 CIE chromaticity coordinate changes from blue (0.15, 0.25) to cyan (0.22, 0.29), white (0.33, 0.38), yellow (0.43, 0.51), and green (0.35, 0.56) with the addition of 0, 0.1, 0.2, 0.5, and 1.0 equiv of Q[8] host to the G1 (10.0 μ M) aqueous solution (pH 2.0) with $\lambda_{ex} = 398$ nm, where X is the chromaticity coordinate that represents the proportion of red primary and Y is the chromaticity coordinate that represents the proportion of green primary.

We present in Scheme 1 a simple and very useful host-guest interaction that results in color-tunable materials. Switching is accomplished by varying the intermolecular assembly of the Q[8] host and cationic guests, OPV derivatives 4,4'-[(1E,1'E)-1,4-phenylenebis(ethene-2,1-diyl)]bis(1-carboxyethylpyridinium)bromide (G1), in aqueous solution. Here, the guest is the chromophore and recognition unit. We achieved color tuning by simple addition of different amounts of Q[8] to a solution of G1, which causes a wide Stokes shift (475–580 nm). The resulting host-guest interactions enabled the creation of cyan, yellow, green, and white emission assemblies in water. Furthermore, the noncovalent interaction led to the fluorescent materials with switchability due to the reversibility of the host-guest inclusion. This dynamical property gives the macrocycle-based host-guest interaction potential applications in smart light-emitting materials.

RESULTS AND DISCUSSION

Cationic aromatic guests are suitable molecules for the stable inclusion of a host-guest interaction for the Q[8] container because of their easy entry into the cavities due to the hydrophobic effect in aqueous media. We thus prepared the ditopic guest 1 (G1) based on the OPV core (Figure S1) of the

host-guest interaction. The propionic acid group was selected as the end unit because this group not only increases the aqueous solubility of G1 but also reversibly switches between neutral and anionic states, depending on the pH of the media. Experimental determination by pH titration showed that the pK_a of G1 is around 4.52 (Figure S2). To maintain the two identical N-substituted carboxylic acid groups in their protonated forms, the host-guest interaction of Q[8] with G1 in aqueous medium at pH 2.0 was first studied (Table S1 and Figure S3). As shown in Figure 1a, the fluorescence spectrum of free G1 in aqueous buffer solution features a blue emission at 475 nm (maximum) upon excitation at 398 nm. Following the addition of 0.5 equiv of Q[8] to the G1 solution, a significant fluorescence red shift with a large Stokes shift (up to 105 nm) and enhancement in the maximum emission peak at 580 nm occurred, and a bright yellow color under UV light was visible. The fluorescence lifetime measurements revealed that the excited-state lifetime of G1 increased remarkably from 0.13 to 18.17 ns (Figures S4) and that the estimated absolute fluorescence quantum yield ($\Phi_{i(abs)}$) value increased from 3.37 to 18.58% upon encapsulation by the Q[8] host (Figure S5). The UV-vis absorption spectrum of G1 also displayed remarkable changes in the presence of Q[8]. As Figure 1b

indicates, with the increasing concentrations of Q[8] up to 0.5 equiv, the maximum absorbance peak of G1 at 390 nm decreased considerably with the bathochromic shift of the band at 400–500 nm. Surprisingly, the absorption peak blue-shifted to 368 nm upon further addition of Q[8]. A plot of absorbance intensity at 450 nm versus n (Q[8]/G1, mole ratio) indicated models of 1:2 and 1:1 binding for the Q[8]/G1 system (Figure 1b). In particular, the noteworthy red shift in the absorption and emission features of the 1:2 model indicated that the J-dimer Q[8]/G1 complexes formed^{39,40} (Figure S6) at lower Q[8] concentrations below 5.0 μ M.

In the light-emitting field, multicolor emissions can be obtained by careful tuning of each color contribution and energy transfer between dye components in the system. For example, white light has been obtained by tuning the contributions of three primary colors (blue, green, and red)^{13,41} or two complementary luminescent colors (blue and yellow).⁴² As a result, much of the research into achieving multicolor luminescence and white emission has been done on the elaborate, trial-and-error tuning of mixing ratios between energy-transferable dyes under specific conditions.^{13,41,43} This approach, however, requires careful design of chromophores to balance the energy transfer between the dyes in the system, as well as repetitive and time-consuming experiments to check the entire emission spectrum for every single mixing ratio of dyes. In this work, compared with the UV absorption peak for the free guest G1 ($\lambda_{\text{max}} = 390$ nm) with blue fluorescence emission ($\lambda_{\text{max}} = 475$ nm), that of Q[8], which triggered dimer complexes under the same conditions and had yellow fluorescence emission ($\lambda_{\text{max}} = 580$ nm), red-shifted the maximum UV absorption peak to 405 nm ($\Delta\lambda = 15$ nm) (Figure 2a). This result indicates that the complementary luminescent colors blue and yellow in white light may be independently obtained at excitation wavelengths between 390 and 405 nm.⁴⁴ As expected, the fluorescence spectrum of G1 shows a typical intense band centered at 475 nm upon excitation at 398 nm (Figure 2b), and the fluorescence intensity decreased with the increase in emission of the J-dimer complex at 580 nm with increased concentrations of Q[8]. This result implies that Q[8] plays an important role in the yellow emission. Detailed results for the normalized overlap spectrum of the fluorescence emission (Figure 2c and Figure S7) suggest that the emission band of G1 in the presence of 0.20 equiv of Q[8] almost encompassed both emission bands of G1 (blue emission) and the J-dimer complex (yellow emission) and covered the entire visible spectral region from 400 to 700 nm. The resulting white-light emission in solution had a $\Phi_{\text{f(abs)}}$ of 12.18% (Figure S5) and a long lifetime at 14.86 ns (Figure S4). However, as the concentrations of added Q[8] exceeded 0.20 equiv of G1, the emission band in this system quickly shifted to the yellow region (580 nm maximum emission), eventually reaching the green region (532 nm maximum emission) (Figure 2b). This observation further supports that white-light emission stems from a balanced mixture of blue emission from free G1 and yellow emission from the gradual Q[8]/G1 (1:2) interaction. The CIE chromaticity diagram shows that the coordinates for the white-light emission are (0.33, 0.38), which are close to those of the emission for pure white light (0.33, 0.33) (Figure 2d). Accordingly, the partial host–guest interaction-induced white-light emission was easily obtained after a change in the amount of Q[8] in aqueous solution at room temperature. Closer inspection suggests more color-tuning emissions can be obtained by the Q[8]/G1 interactions

(Scheme 1 and Figure 2d). This feature makes the discrete macrocyclic receptor-based host–guest system useful for color-tunable materials.

Our study revealed that white-light emission could be obtained by simple addition of a nonfluorescent macrocyclic host to a single guest (blue color emission) solution. The key factor in this system is the host–guest interaction, which triggers yellow color emission with an appropriately ratiometric response for fluorescence intensity. For instance, the maximum fluorescent emission of G1 at 475 nm gradually decreased, and the accompanying maximum fluorescent emission at 580 nm increased with increasing concentrations of Q[8] molecules (Figure 2b) upon excitation at 398 nm. As the Q[8] host controls the intensity ratio of the two emission peaks (blue/yellow, 475/580 nm), the tuning of white light is more accurate and sensitive (Figure S8). In fact, recent ratiometric responses have been interesting because the ratio between the two emission intensities is accurate and is switchable by external stimuli. In particular, a built-in correction for environmental effects such as photobleaching, fluorophore molecule concentration, and the environment around the fluorophore molecule (pH, polarity, temperature, etc.) may be provided.^{45,46} Here, the ratiometric response triggered by the host–guest interaction showed that Q[8] can be potentially used to control precisely the relative intensity ratios of individual emission bands of multicolored luminescence materials in aqueous media. The present work thus complements other works on white-light emission materials that usually require a mixture of two or more independent color components.

Because of its large cavity size and the high negative charge density at its portals, the Q[8] host can probably encapsulate two cationic G1 molecules through multiple ion–dipole interactions, a hydrophobic effect, and HSCT interactions with antiparallel orientations, leading to a noncovalent J-dimer complex.^{31,39} This event probably occurred at initial concentrations of Q[8] (0–0.5 equiv) in the titration procedure in the present study. Thus, the broadening and the initial red shifts in the absorption (Figure 1) and emission spectrum (Figure 2b) may be ascribed to extensive π – π interactions or intermolecular orbital overlap between G1 homodimers in the Q[8] cavity at a Q[8]/G1 stoichiometry of 1:2. The calculated binding constant K_a is $(9.47 \pm 0.56) \times 10^6 \text{ M}^{-2}$ (Figure S9), suggesting that the stronger binding facilitates the stable Q[8]/G1 J-dimer complexes in water.⁴⁷ Therefore, further significant changes in the absorption (maximum absorption at 405 nm visibly decreased and then finally blue-shifted to 368 nm) and emission spectrum (maximum emission at 580 nm gradually increased with the tunable blue shift to 532 nm) at higher Q[8] concentrations (0.5–1.0 equiv) indicate that equilibria of the Q[8]/G1 complexation shifted from the 1:2 complex to the 1:1 assembly. Meanwhile, the unusual multicolor emission triggered by higher concentrations of the Q[8] host is different from the changes observed with the normal 1:1 complexes of Q[n], which showed general enhancement²⁹ or a blue shift^{30a} of fluorescence emission. The host–guest interaction induced further structural changes, and the electronic distributions of G1 are generally ascribed to such novel photophysical properties. In other words, the color tuning achieved at wavelengths of 580–532 nm is partly due to overlapping emissions from the different host–guest complexes and partly due to the different conformational structures of the chromophore in these complexes (Figure S10). Therefore, the 1:1 Q[8]/G1 assembly is not a simple 1:1 monomer host–

guest interaction; a 2:2 cyclic complex (H-dimer) and supramolecular polymers interacting in head-to-tail (chain-like) fashion at a 2:2 Q[8]/G1 mole ratio are more plausible (Figure S11).

On the other hand, pioneering studies suggest that the H-dimer is a poor emitter and that fluorescence quenching generally occurs, whereas J-dimer complexes typically show efficient luminescence.^{35,40} In the present study, the fluorescence lifetime and $\Phi_{\text{f(abs)}}$ of the 1:1 Q[8]/G1 complex were found to be 11.46 ns and 22.17% (Figures S4 and S5), respectively, indicating the J-complex. From a structural viewpoint, formation of 2:2 Q[8]/G1 cyclic complexes may also be prevented by the repulsion between the two cationic OPV moieties due to positive charges. All of these clues strongly suggest a head-to-tail interaction between supramolecular Q[8]/G1 polymers at higher concentrations of Q[8] in aqueous solution (Figure S11). Jiang and co-workers recently proved that tetramethylcucurbit[6]uril (TMeQ[6], which has a cavity smaller than that of Q[8]) can simultaneously encapsulate and bind two *N*-carboxymethyl moieties within its cavity, thus forming porphyrin–TMeQ[6]-based supramolecular polymers.⁴⁸ Thus, we believe that the Q[8] host can also capture two *N*-substituted propionic acid groups in its large hydrophobic cavity.

The above conclusions are supported by results for ¹H NMR titration of Q[8] with G1 in D₂O at pD 2.0 (Figure 3). Upon

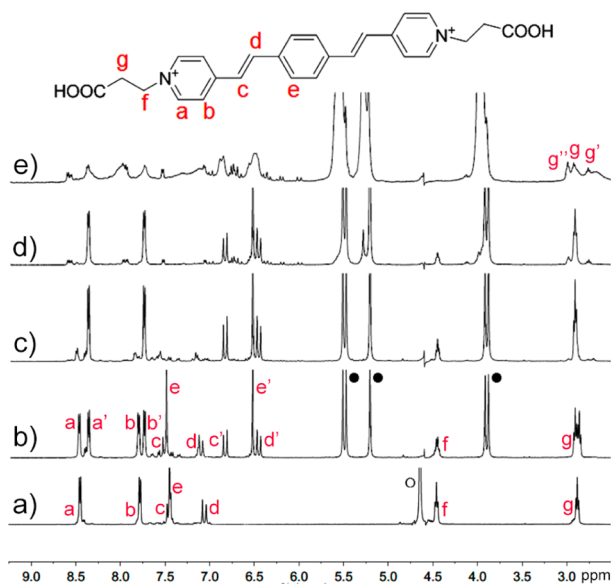


Figure 3. ¹H NMR titration of the Q[8]–G1 system in D₂O (pD 2.0) at 298 K. (a) Resonance signals for the free G1 (1.0 mM). (b–e) Changes in resonance signals of G1 in the presence of 0.25, 0.5, 0.8, and 1.0 equiv of Q[8]. The Q[8] and D₂O protons are labeled as (●) and (○), respectively.

gradual addition of Q[8] (~0.25 equiv) to a solution of G1, resonances corresponding to the protons on the aromatic ring and ethylene of G1 split into two sets of signals, one shifted upfield and one at the original position (Figure 3b). This finding indicates that the complexed and uncomplexed forms of Q[8] and G1 initially coexist in solution, consistent with the fluorescence spectrum for white-light emission, which is derived from the mixture of blue emission of G1 and yellow emission of J-dimer complexes. At increasing concentrations of Q[8] to ~0.5 equiv (Figure 3c), the original proton signal disappeared.

In particular, signals for the protons H_c and H_d of the ethylene moieties and H_e of the center phenyl group shifted obviously upfield from δ 7.46 to 6.86 ppm ($\Delta\delta = 0.60$ ppm), from δ 7.06 to 6.48 ppm ($\Delta\delta = 0.58$ ppm), and from δ 7.44 to 6.55 ppm ($\Delta\delta = 0.99$ ppm), respectively. In contrast, no significant changes in proton chemical shift for *N*-substituted propionic acid (H_g and H_{g'}) were observed. These results suggested that the phenyl and ethylene moieties buried in the Q[8] cavity lead to the formation of stable 1:2 Q[8]/G1 J-dimer complexes. It is plausible that the Q[8] “wheel” is threaded on the G1 “axle” and the Q[8] can move back and forth along the OPV core of G1. Ion–dipole interactions between positively charged nitrogen atoms of the G1 and the carbonyl oxygen atoms of the Q[8] host prevent the Q[8] wheel from dissociating from the G1 axle. This motion is relatively fast on the NMR time scale; thus, all of the signals for the protons on the OPV core shifted upfield in the spectrum (Figure 3c and Figure S12). Notably, OPV protons are still in the same upfield area as multiple resonances appeared, and a new set of protons on the Q[8] host were observed when concentrations of Q[8] added to the G1 solution increased up to ~1.0 equiv (Figure 3d,e and Figure S12). This finding further implies that the host–guest interaction between Q[8] and G1 relies on the initial 1:2 structure. Furthermore, protons on the *N*-substituted propionic acid also underwent interesting changes in this procedure. For example, the signals for some H_g protons shifted upfield (H_g^u) and some downfield (H_g^d), and even some stayed in the original position (H_g). These results suggest that some protons were in the Q[8] cavity (upfield shift due to the shielding effect of the hydrophobic cavity) and that some were on or near the Q[8] portal (downfield shift due to the deshielding effect of the carbonyl-rimmed portal). They thus confirm the proposed head-to-tail chain-like supramolecular polymers at a high concentration of Q[8] (Scheme 1).

To further verify these conclusions, dynamic light scattering (DLS) experiments were performed to examine the size distributions of the host–guest recognition induced by the two discrete assemblies in solution. Q[8] (10.0 μ M) and G1 (10.0 μ M) in aqueous solution at pH 2.0 exhibited average hydrodynamic diameters of 530 nm (Figure S13a), which indicated the existence of supramolecular polymer chains. Atomic force microscopy studies also showed the formation of linear 1D supramolecular polymers from a concentrated equimolar solution of Q[8] and G1 (Figure S13c). For comparison, the structure of the 1:2 Q[8]/G1 complex under the same conditions was determined. We found that the host–guest complex has a center hydrodynamic diameter of 4.0 nm (Figure S13b), indicating the formation of J-dimer complexes.

In the light-emitting field, aggregation of luminophores generally has two different effects on emission: aggregation-caused quenching (ACQ) and aggregation-induced emission (AIE). The former is often self-quenching at high concentrations, and the latter falls dark when aggregation is disrupted.¹⁴ Interestingly, the photoluminescence properties of the host–guest induced emission (HGIE) system in the present study displayed longer fluorescence lifetime and higher quantum yield (Figures S4 and S5) in both dilute (10^{−6} M) and high (10^{−4} M) concentrations of the complexes. This result suggests that the HGIE system may serve as a new type of chromophore in light-emitting materials (Figures S14 and S15). For comparison, similarly water-soluble macrocyclic hosts β - and γ -cyclodextrin were introduced in place of Q[8] to the G1 solution under the same conditions (Figure S16). No

significant fluorescence emission changes were observed; thus, the Q[8] as the macrocyclic host offers a unique advantage in fabricating smart color-tuning materials.

Supramolecular pK_a shifts, especially those due to macrocyclic complexation of guests, have recently attracted significant attention in catalytic and biomimetic chemistry.⁴⁹ Q[n]s have been shown to significantly shift the pK_a values of encapsulated guests relative to those of the macrocyclic host and have been exploited in the development of reporters for fluorescent assaying, sensing, supramolecular catalysis, activation, and prodrug stabilization.^{50,51} In the present study, the host–guest interaction resulted in a narrow shift of the G1 pK_a from 4.52 to 5.48 ($\Delta pK_a = 0.96$) (Figure S17). Interestingly, our study features unusual dynamical photophysical properties of the narrow pK_a shift. As shown in Figure 4, the maximal

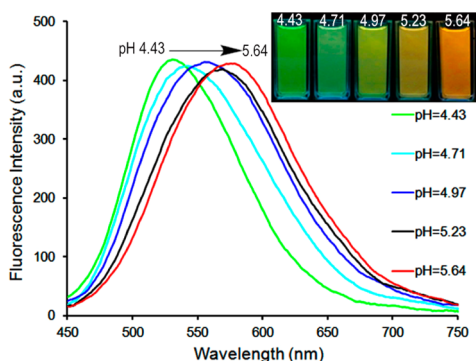


Figure 4. pH-Dependent tunable emissions. Tunable luminescence due to two coexisting host–guest interactions between Q[8] and G1 at pH 4.6–5.5. The luminescence, which is due to the host-assisted pK_a shift, ultimately results in distinguishable profiles of fluorescent emissions due to minor pH changes ($\lambda_{ex} = 398$ nm).

emission peaks of G1 gradually red-shifted the pH between ~4.4 and 5.6: shifts to 529, 538, 558, 567, and 580 nm accompanied pH changes to 4.43, 4.71, 4.97, 5.23, and 5.64, respectively. The tunable fluorescence response associated with the host-assisted pK_a shift of G1 is expected to occur between the pK_a values for the J-dimer complexes (1:2 Q[8]/G1) and chain-like polymers (1:1, Q[8]/G1), that is, between pH 4.6 and 5.5. In this pH range, a large fraction of the chain-like polymers with the protonated $-\text{COOH}$ moiety collapse and converted into J-dimer complexes with the deprotonated $-\text{COO}^-$ moiety (Figure S18), which is very similar to the reversible fluorescence emission changes of G1 at the high concentration of Q[8] at pH 2.0 (Figure 2b). These noteworthy changes in the fluorescence emission features indicate that the Q[8]/G1 system in aqueous solution has potential application as a fluorescent pH sensor for accurate, narrow pH changes (0.1–0.2) in environmental and biological studies.⁵²

Kaifer and co-workers reported that protonation and deprotonation of the two-terminal COOH groups on a 4,4'-bipyridinium linear derivative lead to pronounced switching between a molecular shuttle and molecular pseudorotaxanes in Q[n] chemistry.⁵³ A crucial factor for this phenomenon is the presence of substantial electrostatic repulsions between the carboxylate negative charges on the ends of the axle component and the carbonyl oxygens on the two identical portals of Q[n]s. In line with this observation, we hypothesize that the reversible Q[8]/G1 assembly in the present study may also be controlled

through acid–base titration of the two-terminal COOH groups. In particular, the chain-like Q[8]/G1 supramolecular polymers would be essentially inhibited due to the electrostatic repulsions between the anionic carboxylate forms and Q[8] portals (Figure S19). As expected, UV–vis absorption (Figure S20), fluorescence emission spectrum (Figure S21), and DLS analysis data (Figure S22) for G1 and Q[8] at higher pH value (7.2) indicate that a head-to-tail supramolecular polymer did not exist even at a high concentration of Q[8]. We further elucidated the host–guest interaction from the isothermal titration calorimetry (ITC) data, which revealed a 1:2 stoichiometry with binding constant $K_a = (2.50 \pm 0.16) \times 10^6 \text{ M}^{-2}$ (Figure S23). This result implies that only the J-dimer complex was stably formed at higher pH values.

CONCLUSIONS

In summary, a facile Q[8]-based supramolecular approach to fabricate dynamically smart luminescent materials in aqueous solution is described. This approach greatly decreased the number of required synthetic steps and produced a system with tunable and reversible photophysical properties. The host–guest interaction based on the macrocyclic container was produced by simple addition of Q[8] to a solution of G1. It provides a toolbox for producing cyan, yellow, green, and white fluorescent emissions. Furthermore, the host–guest interaction, which triggers ratiometric fluorescence responses between blue and yellow emissions, provides evidence that may be used for obtaining pure white-light emission by control of supramolecular assemblies with lower cost. The emission induced by the host–guest interaction is substantially different from those of ACQ and AIE chromophores, the fluorescence emission enhancement that occurs at both low and high concentration with long lifetime and high quantum yield. Such emission properties indicate a wider application of a Q[8]-based supramolecular approach in light-emitting materials.

ASSOCIATED CONTENT

Supporting Information

The Supporting Information is available free of charge on the ACS Publications website at DOI: 10.1021/jacs.6b01223.

Full experimental details, NMR, UV–vis, fluorescence spectrum, fluorescence lifetime, estimated absolute fluorescence quantum yield, ITC experiment, and control experiments (PDF)

AUTHOR INFORMATION

Corresponding Author

*longni333@163.com

Notes

The authors declare no competing financial interest.

ACKNOWLEDGMENTS

This work was supported by the Natural Sciences Foundation of China (No. 21302026) and the Student's Platform for Innovation and Entrepreneurship Training Program (No. 201510657019).

REFERENCES

- (1) Yang, S. K.; Shi, X.; Park, S.; Ha, T.; Zimmerman, S. C. *Nat. Chem.* **2013**, *5*, 692–697.
- (2) Yang, Z.; Cao, J.; He, Y.; Yang, J. H.; Kim, T.; Peng, X.; Kim, J. S. *Chem. Soc. Rev.* **2014**, *43*, 4563–4601.

- (3) Stender, A. S.; Marchuk, K.; Liu, C.; Sander, S.; Meyer, M. W.; Smith, E. A. *Chem. Rev.* **2013**, *113*, 2469–2527.
- (4) Zhu, M.; Yang, C. *Chem. Soc. Rev.* **2013**, *42*, 4963–4976.
- (5) Maggini, L.; Bonifazi, D. *Chem. Soc. Rev.* **2012**, *41*, 211–241.
- (6) Bura, T.; Retailleau, P.; Ziessel, R. *Angew. Chem., Int. Ed.* **2010**, *49*, 6659–6663.
- (7) Oh, J.-W.; Lee, Y. O.; Kim, T. H.; Ko, K. C.; Lee, J. Y.; Kim, H.; Kim, J. S. *Angew. Chem., Int. Ed.* **2009**, *48*, 2522–2524.
- (8) Figueira-Duarte, T. M.; Simon, S. C.; Wagner, M.; Druzhinin, S. I.; Zachariasse, K. A.; Müllen, K. *Angew. Chem., Int. Ed.* **2008**, *47*, 10175–10178.
- (9) Frath, D.; Massue, J.; Ulrich, G.; Ziessel, R. *Angew. Chem., Int. Ed.* **2014**, *53*, 2290–2310.
- (10) Figueira-Duarte, T. M.; Müllen, K. *Chem. Rev.* **2011**, *111*, 7260–7314.
- (11) Aida, T.; Meijer, E. W.; Stupp, S. I. *Science* **2012**, *335*, 813–817.
- (12) Po, C.; Tam, A. Y.-Y.; Wong, K. M.-C.; Yam, V. W.-W. *J. Am. Chem. Soc.* **2011**, *133*, 12136–12143.
- (13) Abbel, R.; Grenier, C.; Pouderoijen, M. J.; Stouwdam, J. W.; Leclère, P. E. L. G.; Sijbesma, R. P.; Meijer, E. W.; Schenning, A. P. H. *J. Am. Chem. Soc.* **2009**, *131*, 833–843.
- (14) Hong, Y.; Lam, J. W. Y.; Tang, B. Z. *Chem. Soc. Rev.* **2011**, *40*, 5361–5388.
- (15) Zhang, X.; Rehm, S.; Safont-Sempere, M. M.; Würthner, F. *Nat. Chem.* **2009**, *1*, 623–629.
- (16) An, B.-K.; Gihm, S. H.; Chung, J. W.; Park, C. R.; Kwon, S.-K.; Park, S. Y. *J. Am. Chem. Soc.* **2009**, *131*, 3950–3957.
- (17) Pollock, J. B.; Schneider, G. L.; Cook, T. R.; Davies, A. S.; Stang, P. J. *J. Am. Chem. Soc.* **2013**, *135*, 13676–13679.
- (18) Yan, X.; Cook, T. R.; Wang, P.; Huang, F.; Stang, P. J. *Nat. Chem.* **2015**, *7*, 342–348.
- (19) Babu, S. S.; Praveen, V. K.; Ajayaghosh, A. *Chem. Rev.* **2014**, *114*, 1973–2129.
- (20) Sagara, Y.; Kato, T. *Nat. Chem.* **2009**, *1*, 605–610.
- (21) (a) Kim, J.; Jung, I. S.; Kim, S. Y.; Lee, E.; Kang, J. K.; Sakamoto, S.; Yamaguchi, K.; Kim, K. *J. Am. Chem. Soc.* **2000**, *122*, 540–541. (b) Day, A. I.; Blanch, R. J.; Arnold, A. P.; Lorenzo, S.; Lewis, G. R.; Dance, I. A. *Angew. Chem., Int. Ed.* **2002**, *41*, 275–277. (c) Cheng, X. J.; Liang, L. L.; Chen, K.; Ji, N. N.; Xiao, X.; Zhang, J. X.; Zhang, Y. Q.; Xue, S. F.; Zhu, Q. J.; Ni, X. L.; Tao, Z. *Angew. Chem., Int. Ed.* **2013**, *52*, 7252–7255.
- (22) (a) Shetty, D.; Khedkar, J. K.; Park, K. M.; Kim, K. *Chem. Soc. Rev.* **2015**, *44*, 8747–8761. (b) Assaf, K. I.; Nau, W. M. *Chem. Soc. Rev.* **2015**, *44*, 394–418. (c) Ni, X.-L.; Xiao, X.; Cong, H.; Liang, L.-L.; Cheng, K.; Cheng, X.-J.; Ji, N.-N.; Zhu, Q.-J.; Xue, S.-F.; Tao, Z. *Chem. Soc. Rev.* **2013**, *42*, 9480–9508. (d) Lagona, J.; Mukhopadhyay, P.; Chakrabarti, S.; Isaacs, L. *Angew. Chem., Int. Ed.* **2005**, *44*, 4844–4870.
- (23) (a) Yu, G.; Jie, K.; Huang, F. *Chem. Rev.* **2015**, *115*, 7240–7303. (b) Liu, Y. L.; Yang, H.; Wang, Z. Q.; Zhang, X. *Chem. - Asian J.* **2013**, *8*, 1626–1632.
- (24) (a) Lee, D.-W.; Park, K. M.; Banerjee, M.; Ha, S. H.; Lee, T.; Suh, K.; Paul, S.; Jung, H.; Kim, J.; Selvapalam, N.; Ryu, S. H.; Kim, K. *Nat. Chem.* **2011**, *3*, 154–159. (b) Gong, B.; Choi, B.-K.; Kim, J.-Y.; Shetty, D.; Ko, Y. H.; Selvapalam, N.; Lee, N. K.; Kim, K. *J. Am. Chem. Soc.* **2015**, *137*, 8908–8911.
- (25) (a) Ma, D.; Hettiarachchi, G.; Nguyen, D.; Zhang, B.; Wittenberg, J. B.; Zavalij, P. Y.; Briken, V.; Isaacs, L. *Nat. Chem.* **2012**, *4*, 503–510. (b) Isaacs, L. *Acc. Chem. Res.* **2014**, *47*, 2052–2062.
- (26) (a) Lee, T.-C.; Kalenius, E.; Lazar, A. I.; Assaf, K. I.; Kuhnert, N.; Grün, C. H.; Jänis, J.; Scherman, O. A.; Nau, W. M. *Nat. Chem.* **2013**, *5*, 376–382. (b) Kaifer, A. E. *Acc. Chem. Res.* **2014**, *47*, 2160–2167. (c) Ni, X.-L.; Xiao, X.; Cong, H.; Zhu, Q.-J.; Xue, S.-F.; Tao, Z. *Acc. Chem. Res.* **2014**, *47*, 1386–1395.
- (27) (a) Hou, X.; Ke, C.; Bruns, C. J.; McGonigal, P. R.; Pettman, R. B.; Stoddart, J. F. *Nat. Commun.* **2015**, *6*, 6884. (b) Jiao, Y.; Liu, K.; Wang, G.; Wang, Y.; Zhang, X. *Chem. Sci.* **2015**, *6*, 3975–3980. (c) Smith, L. C.; Leach, D. G.; Blaylock, B. E.; Ali, O. A.; Urbach, A. R. *J. Am. Chem. Soc.* **2015**, *137*, 3663–3669. (d) Joseph, R.; Nkrumah, A.; Clark, R. J.; Masson, E. *J. Am. Chem. Soc.* **2014**, *136*, 6602–6607.
- (e) Chen, K.; Kang, Y.-S.; Zhao, Y.; Yang, J.-M.; Lu, Y.; Sun, W.-Y. *J. Am. Chem. Soc.* **2014**, *136*, 16744–16747. (f) Zhang, Q.; Tian, H. *Angew. Chem., Int. Ed.* **2014**, *53*, 10582–10584. (g) Liu, K.; Liu, Y.; Yao, Y.; Yuan, H.; Wang, S.; Wang, Z.; Zhang, X. *Angew. Chem., Int. Ed.* **2013**, *52*, 8285–8289.
- (28) Ghale, G.; Nau, W. M. *Acc. Chem. Res.* **2014**, *47*, 2150–2159.
- (29) Choudhury, S. D.; Mohanty, J.; Pal, H.; Bhasikuttan, A. C. *J. Am. Chem. Soc.* **2010**, *132*, 1395–1401.
- (30) (a) Freitag, M.; Gundlach, L.; Piotrowiak, P.; Galoppini, E. *J. Am. Chem. Soc.* **2012**, *134*, 3358–3366. (b) Ryan, S. T. J.; Del Barrio, J.; Ghosh, I.; Biedermann, F.; Lazar, A. I.; Lan, Y.; Coulston, R. J.; Nau, W. M.; Scherman, O. A. *J. Am. Chem. Soc.* **2014**, *136*, 9053–9060.
- (31) Ko, Y. H.; Kim, E.; Hwang, I.; Kim, K. *Chem. Commun.* **2007**, 1305–1315.
- (32) Zhang, J.; Coulston, R. J.; Jones, S. T.; Geng, J.; Scherman, O. A.; Abell, C. *Science* **2012**, *335*, 690–694.
- (33) Huang, Z.; Yang, L.; Liu, Y.; Wang, Z.; Scherman, O. A.; Zhang, X. *Angew. Chem., Int. Ed.* **2014**, *53*, 5351–5355.
- (34) (a) Tian, J.; Zhou, T.-Y.; Zhang, S.-C.; Aloni, S.; Altoe, M. V.; Xie, S.-H.; Wang, H.; Zhang, D.-W.; Zhao, X.; Liu, Y.; Li, Z.-T. *Nat. Commun.* **2014**, *5*, 5574. (b) Zhang, K.-D.; Tian, J.; Hanifi, D.; Zhang, Y.; Sue, A. C.-H.; Zhou, T.-Y.; Zhang, L.; Zhao, X.; Liu, Y.; Li, Z.-T. *J. Am. Chem. Soc.* **2013**, *135*, 17913–17918.
- (35) Barooah, N.; Mohanty, J.; Bhasikuttan, A. C. *Chem. Commun.* **2015**, *51*, 13225–13228.
- (36) Ajayaghosh, A.; Praveen, V. K. *Acc. Chem. Res.* **2007**, *40*, 644–656.
- (37) Praveen, V. K.; Ranjith, C.; Bandini, E.; Ajayaghosh, A.; Armaroli, N. *Chem. Soc. Rev.* **2014**, *43*, 4222–4242.
- (38) Vijayakumar, C.; Praveen, V. K.; Ajayaghosh, A. *Adv. Mater.* **2009**, *21*, 2059–2063.
- (39) Pattabiraman, M.; Natarajan, A.; Kaliappan, R.; Mague, J. T.; Ramamurthy, V. *Chem. Commun.* **2005**, 4542–4544.
- (40) Würthner, F.; Kaiser, T. E.; Saha-Möller, C. R. *Angew. Chem., Int. Ed.* **2011**, *50*, 3376–3410.
- (41) Giansante, C.; Raffy, G.; Schäfer, C.; Rahma, H.; Kao, M.-T.; Olive, A. G. L.; Del Guerso, A. *J. Am. Chem. Soc.* **2011**, *133*, 316–325.
- (42) Gong, Q.; Hu, Z.; Deibert, B. J.; Emge, T. J.; Teat, S. J.; Banerjee, D.; Mussman, B.; Rudd, N. D.; Li, J. *J. Am. Chem. Soc.* **2014**, *136*, 16724–16727.
- (43) (a) Babu, S. S.; Aimi, J.; Ozawa, H.; Shirahata, N.; Saeki, A.; Seki, S.; Ajayaghosh, A.; Mohwald, H.; Nakanishi, T. *Angew. Chem., Int. Ed.* **2012**, *51*, 3391–3395. (b) Rao, K. V.; Datta, K. K. R.; Eswaramoorthy, M.; George, S. J. *Adv. Mater.* **2013**, *25*, 1713–1718.
- (44) Kasha, M. *Discuss. Faraday Soc.* **1950**, *9*, 14–19.
- (45) Tsien, R. Y.; Harootunian, A. T. *Cell Calcium* **1990**, *11*, 93–109.
- (46) Fan, J.; Hu, M.; Zhan, P.; Peng, X. *Chem. Soc. Rev.* **2013**, *42*, 29–43.
- (47) Masson, E.; Ling, X.; Joseph, R.; Kyeremeh-Mensah, L.; Lu, X. *RSC Adv.* **2012**, *2*, 1213–1247.
- (48) Xiao, X.; Sun, J.; Jiang, J. *Chem. - Eur. J.* **2013**, *19*, 16891–16896.
- (49) Pluth, M. D.; Bergman, R. G.; Raymond, K. N. *Science* **2007**, *316*, 85–88.
- (50) Praetorius, A.; Bailey, D. M.; Schwarzlose, T.; Nau, W. M. *Org. Lett.* **2008**, *10*, 4089–4092.
- (51) Saleh, N.; Koner, A. L.; Nau, W. M. *Angew. Chem., Int. Ed.* **2008**, *47*, 5398–5401.
- (52) Cogan, M. G. *Fluid and Electrolytes*; Appleton and Lange-Prentice Hall Publishers: Norwalk, CT, 1991.
- (53) Kaifer, A. E.; Li, W.; Silvi, S.; Sindelar, V. *Chem. Commun.* **2012**, *48*, 6693–6695.